4036 *J. Phys. Chem. B* **2008,** *112,* 4036−4047

Monte Carlo Simulation of Electrodeposition of Copper: A Multistep Free Energy Calculation

S. Harinipriya and Venkat R. Subramanian*

Department of Chemical Engineering, Tennessee Technological University, Cookeville, Tennessee 38505

Received: August 2, 2007; In Final Form: December 22, 2007

Electrodeposition of copper (Cu) involves length scales of a micrometer or even less. Several theoretical techniques such as continuum Monte Carlo, kinetic Monte Carlo (KMC), and molecular dynamics have been used for simulating this problem. However the multiphenomena characteristics of the problem pose a challenge for an efficient simulation algorithm. Traditional KMC methods are slow, especially when modeling surface diffusion with large number of particles and frequent particle jumps. Parameter estimation involving thousands of KMC runs is very time-consuming. Thus a less time-consuming and novel multistep continuum Monte Carlo simulation is carried out to evaluate the step wise free energy change in the process of electrochemical copper deposition. The procedure involves separate Monte Carlo codes employing different random number criterion (using hydrated radii, bare radii, hydration number of the species, redox potentials, etc.) to obtain the number of species ($CuCl_2$ or $CuSO_4$ or Cu as the case may be) and in turn the free energy. The effect of concentration of electrolyte, influence of electric field and presence of chloride ions on the free energy change for the processes is studied. The rate determining step for the process of electrodeposition of copper from $CuCl_2$ and $CuSO_4$ is also determined.

1. Introduction

An electrochemical interface is defined as a phase boundary between a metal and a liquid.[1] The structural dynamics of such an ubiquitous interface is important in the field of metal electrodeposition.[2] The extensive knowledge of interfacial dynamics and structure would direct the a priori solution to the problems existing in the process of electrodeposition.[3] Electrodeposition plays a vital role in applications like thin films,[4−6] microelectronics,[7−9] microelectromechanical systems,[10] and nanofabrication.[11−13] Electrodeposition of metals has several aspects that complement the aforementioned fields such as (i) control of deposition thickness precisely to nanometer scale,[14] (ii) the reversibility of the phenomena for most of the metals,[8] and (iii) attaining complex structures like two-dimensional[8] (2-D) and three-dimensional[8] (3-D) topographies that are difficult to achieve via conventional fabrication techniques. Recent works on electrodeposition primarily focus on copper (Cu) deposition[14] which involves length scales of a micrometer or even less. This importance to copper can be attributed to (i) the large conductivity of Cu relative to other metals,[9,15] (ii) better electromigration,[15] and (iii) cost effectiveness.[15] For these persuasive reasons, more research is done on perfecting Cu electroplating.[16] The copper electrodeposition plays a major role in applications such as (i) production of protective coatings and/or decorative coatings on diverse substrates,[17] (ii) production of alloys having compositions difficult to attain through other production methods,[18] and (iii) the synthesis of tailor-made nanoparticles,[19] having ad-hoc properties and dimensions. Copper has become the metal of choice for interconnects, replacing aluminum,[20] because of the performance of integrated circuits, reliability improvement, electromigration, resistance of interconnects, and reduction of interconnect delay time.[19,21] At present, copper is used as an interconnect material due to its high electrical conductivity and higher electromigration. In general, copper is deposited by an electroplating process, due to the competence in depositing several hundred micrometer thick metal layers.[22] In comparison to other physical deposition processes[23,24] such as sputtering, E-beam evaporation, and chemical vapor deposition, the electroplating process is cheaper and faster and requires lower temperatures. It is a known fact that the copper deposits obtained at high current densities and overpotentials are technologically important.[25] Copper deposits with open and porous structures obtained at high current densities are used as electrodes in electrochemical devices[25,26] such as fuel cells, batteries, and chemical sensors, whereas those of high surface area are appropriate for evaluating electrochemical reactions such as nitrate ion reduction[27] and for the reaction in which nitrate is reduced to ammonia (high yield) in the presence of aqueous acidic perchlorate and sulfate media.[28] As the dimensions of copper structures continue to scale down into the nanometer range, the initial stage of copper electroformation, i.e., nucleation, becomes increasingly important.[29] Nucleation can be regarded as a critical stage of growth for definition of the final film properties. Copper nucleation mechanisms have been investigated on substrates such as vitreous carbon,[30−32] sputtered TiN,[33] and copper,[34] from solutions containing sulfates,[30] pyrophosphate,[34] and fluoroborate.[33] In addition, it was found that the type of nucleation mechanism is highly dependent on the solution pH and the presence of a supporting electrolyte.[30] Electrodeposition processes of copper involve electrochemical reactions and diffusion at different time scales.[35] Copper ion is transported by convection, bulk diffusion, and migration to the substrate and then deposited on the substrate through electrochemical reactions. Several theoretical techniques such as continuum Monte Carlo,[36−37] kinetic Monte Carlo[38−45] (KMC), and molecular dynamics[46−50] have been used for simulation of these problems. The current state of the art of a continuum

* To whom correspondence should be addressed. E-mail: vsubramanian@tntech.edu. Fax: 931-372-6352. Tel: 931-372-3494.

10.1021/jp076191a CCC: $40.75 © 2008 American Chemical Society
Published on Web 03/07/2008

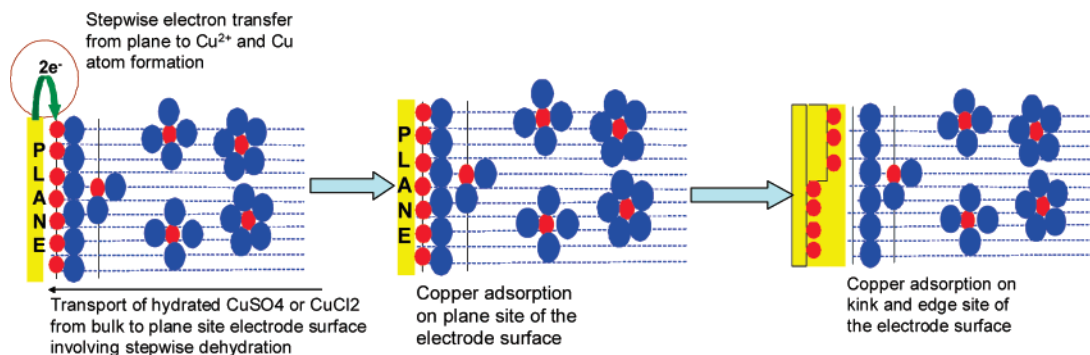

Figure 1. Illustrative representation of the processes involved in the electrochemical deposition of copper on the electrode surface. Blue circles represent the water molecules, hydrated orange circles represent the $CuCl_2$ or $CuSO_4$ molecules (as the case may be), orange circles denote the Cu atoms and the yellow bars indicate the metal electrode surface.

model describes the diffusion, migration, and homogeneous chemical reactions in the bulk electrolyte coupled with phenomenological expressions that take into account transport and electrochemical reactions on the metal/electrolyte interface.

In this article, a methodology is proposed for the estimation of free energy changes involved in the various steps of copper deposition via multistep Monte Carlo simulation. First step is the calculation of the free energy change involved in the dehydration of a hydrated molecule ($CuCl_2$ or $CuSO_4$) while being transported to the metal/electrolyte interface from bulk of the solution. Here the hydrated molecule is considered as an entity and the molecular radii are written as a sum of the cationic and anionic radii based on the hard sphere model. The second step involves the stepwise electron-transfer process leading to Cu atom and subsequent adsorption of Cu on the plane site of the electrode. The third step is the surface diffusion of the Cu atoms from plane to kink to edge sites of the electrode. All of the steps are interconnected by separate continuum Monte Carlo codes that generate random numbers by employing appropriate criterion.

2. Methodology

The present simulation methodology requires input parameters such as (i) the molecular radii of $CuCl_2$ or $CuSO_4$ (assumed as hard spheres), obtained as the sum of cationic and anionic radii, (ii) the radius of water molecules, and (iii) the standard redox potentials of the reactions (a) $Cu^{2+} + e \leftrightarrow Cu^+$ and (b) $Cu^+ + e \leftrightarrow Cu$. Using the first two parameters, the hydration number of the molecules at infinite dilution and, subsequently, the hydration number at a chosen concentration by incorporating the random distribution of species are formulated. Figure 1 depicts the visualization of the processes involved in the electrochemical deposition of copper.

2.1. Simulation Details. The simulation was carried out in the NTP ensemble and the system (consisting of hydrated $CuCl_2$ or $CuSO_4$ assumed as hard spheres) was placed in a cubic box of length l (Å; cf. Figure 2). Boundary conditions are (i) $d_{\text{total}(n)} = d_{\text{total}(n-1)} - X_n$, where X_n is the distance the molecule moved in each step, $d_{\text{total}(n)}$ is the total distance the molecule has to travel from the bulk to the interface, and $d_{\text{total}(n-1)}$ is the remaining distance the molecule has to travel to reach the interface after each step displacement; here $n = 1$ to n_{final}; (ii) $R_n^{\text{hyd}} = R_i + 1$, R_i being the bare molecular radii and R_n^{hyd} is the hydrated radii of the molecule at the nth step of its movement; were employed and the cube was confined (rigidly fixed) along the z axis. The molecules were initially placed at the center of the cube and allowed to move in the direction of the electrode, in the present case along the x axis. The distance (d_{total}) traveled

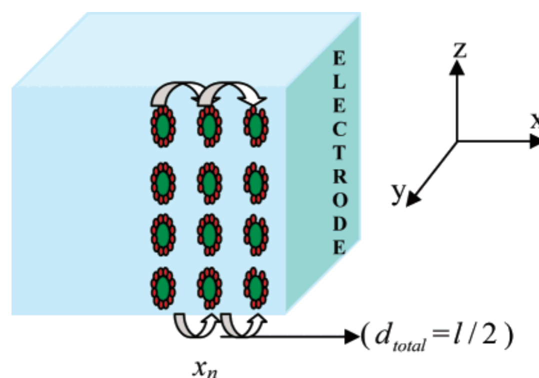

Figure 2. Actual displacement of hydrated $CuCl_2$ or $CuSO_4$. Red circle indicates the water molecules surrounding the $CuCl_2$ or $CuSO_4$ (depicted as green circle); black arrow denotes the direction of movement of the hydrated molecule and x_n being the displacement made by the molecule in each step.

by the molecules will be half the length of the cube ($d_{\text{total}} = l/2$). The simulation was performed for appropriate densities (g/cm^3) of the copper solution. For simplicity, the electrode is assumed to be a smooth copper surface devoid of any anisotropy.

2.2. Input Parameters. *(a) Hydration Number at a Chosen Concentration, Nh_c.* The hydration number at a particular concentration is denoted as Nh_c. For any ionic pair $M_{\nu+}^{z+}X_{\nu-}^{z-}$ in water, $Nh_c < Nh_\infty$, Nh_∞ being the hydration number at infinite dilution. Hence

$$Nh_c = Nh_\infty - \Delta Nh_{total} \tag{1}$$

where ΔNh_{total} indicates the total change in hydration number of the ionic pair between infinite dilution and a chosen concentration.[51]

(i) Total Change in the Hydration Number, ΔNh_{total}. ΔNh_{total} depends upon (i) the dimensions of solvent (water) molecules, d_s, (ii) the mean nearest neighbor distance between two hydrated ionic pairs, $\langle r \rangle$, and (iii) the magnitude of the hydration number at infinite dilution. ΔNh_{total} is directly proportional to d_s (since the extent of desolvation increases with the size of the solvent molecules) and inversely proportional to $\langle r \rangle$ (when $\langle r \rangle \to \infty$, more solvent molecules will surround an ionic pair and hence the number of solvent molecules shed by an ionic pair decreases). Consequently,[51] the expressions obtained are

$$\Delta Nh_{\text{total}} = \frac{Nh_\infty d_s}{\langle r \rangle} \tag{2}$$

Hence

$$Nh_c = Nh_\infty\left(1 - \frac{d_s}{\langle r\rangle}\right) \quad (3)$$

In eq 3, when $\langle r\rangle \rightarrow \infty$ (limit of infinite dilution) the ratio $d_s/\langle r\rangle$ becomes negligible and $Nh_c \approx Nh_\infty$. To obtain Nh_c, the estimates of Nh_∞ and $\langle r\rangle$ need to be evaluated.

(ii) Hydration Number at Infinite Dilution, Nh_∞. The hydration number of an ion at infinite dilution is written as[52]

$$Nh_\infty = \frac{V_{ion}}{V_{water}} \quad (4)$$

where V_{ion} and V_{water} denote the volume of the bare ion and that of water molecules. In the present case, the ionic pair ($Cu^{2+}Cl_2^{2-}$) is considered as an entity, its hydration number at infinite dilution may be represented as[52]

$$Nh_\infty = \frac{(\nu_+ z_+ r_+^{\ 3} + \nu_- z_- r_-^{\ 3})}{r_s^{\ 3}} \quad (5)$$

where r_+ and r_- represent the bare crystallographic radii of the ionic species Cu^{2+} and Cl^- (or SO_4^{2-} as the case may be), ν_+ and ν_- being the stoichiometric number of Cu^{2+} and Cl^- (or SO_4^{2-} as the case may be), while r_s is the radius of water molecules, whereas z_+ and z_- denote the charge on the cation and anion, respectively.

2.3. Mean Nearest Neighbor Distance $\langle r\rangle$. The explicit equation reported by Fritsch et al.[54] for $\langle r\rangle$ in the case of hard spheres is given by

$$\langle r\rangle = \left(\frac{3}{4\pi c}\right)^{1/3} \exp(\eta)[\Gamma(4/3) - b] \quad (6)$$

where

$$b = \sum_{m=0}^{\infty} \frac{(-1)^n \eta^{(m+4/3)}}{m!(m + 4/3)} \quad (7)$$

and the dimensionless density η is defined as

$$\eta = \frac{4\pi c d_{desol}^{\ 3}}{3} \quad (8)$$

c is taken as the concentration of the ionic pair ($Cu^{2+}Cl_2^{2-}$ or $Cu^{2+}SO_4^{2-}$) in molecules/Å^3 and $\Gamma(4/3)$ denotes the Gamma function, d_{desol} being the bare crystallographic diameter of the species under consideration. The evaluation of the mean nearest neighbor distance plays a crucial role in several physiochemical processes like hopping conduction[53] electron-transfer reactions,[54] random walk phenomenon,[55] etc., where the distribution of the species in the dimensionality of interest is important. Since the present case of copper electrodeposition involves electron transfer, distribution of species in a confined cubic simulation box, evaluation of $\langle r\rangle$ becomes inevitable. Employing eqs 2−8 in eq 1, the hydration number of any species at a chosen concentration can be easily evaluated.

2.4. Hydrated Radii of $\nu_+M^{z+}\nu_-X^{z-}$. The hydrated radius R^{hyd} is always greater than the bare radius (R_{desol}) of any ionic pair$\nu_+M^{z+}\nu_-X^{z-}$. Hence

$$R^{hyd} = R_i + R_{excess} \quad (9)$$

where R_i and R_{excess} denotes the bare crystallographic radius and the excess radius gained by the species on account of hydration respectively. R_{excess} may be written as

$$R_{excess} = \gamma r_s \quad (10)$$

and γ is the dimensionless factor that depends on the hydration number of $\nu_+M^{z+}\nu_-X^{z-}$ at infinite dilution (Nh_∞) as well as that at a chosen concentration (Nh_c). It can be represented[51] as the ratio between the hydration number at a chosen concentration (Nh_c) and the total change in hydration number (ΔNh_{total}). Thus

$$\gamma = \frac{Nh_c}{\Delta Nh_{total}} \quad (11)$$

Hence

$$R_{excess} = r_s \frac{Nh_c}{\Delta Nh_{total}} \quad (12)$$

and the hydrated radius of the ionic pair $\nu_+M^{z+}\nu_-X^{z-}$ is written as

$$R^{hyd} = R_i + r_s \frac{Nh_c}{\Delta Nh_{total}} \quad (13)$$

Equation 13 can now be employed to obtain the hydrated radius of $\nu_+ M^{z+}\nu_-X^{z-}$ at a chosen concentration.

The justification of the postulated expressions for Nh_c in terms of ΔNh_{total} and Nh_∞ and R^{hyd} in terms of Nh_c, ΔNh_{total}, r_s, and R_i is demonstrated elsewhere[51] by employing to determine the hydration number at a particular concentration and hydrated radii for alkali metal halides, alkaline-earth metal halides, lanthanum and actinium metal halides, and most inner transition metal halides.

3. Generation of Random Numbers and the Criterion Employed

In order to obtain the number of $CuCl_2$ or $CuSO_4$ molecules that reach the electrode surface, the central molecules are allowed to move in steps (Figure 1). Random numbers are generated for estimating the number of molecules that have reached the subsequent steps. To generate random numbers pertaining to each step, the parameters such as hydration number of $\nu_+M^{z+}\nu_-X^{z-}$ (Nh_{cn}), the hydrated radius (R_n^{hyd}) and the corresponding decrease in the hydration number due to movement of the molecule (ΔNh_n) need to be evaluated. Since the surface of the cube is confined

$$d_{total(n)} = d_{total(n-1)} - x_n \quad (15)$$

$$R_n^{hyd} = R_{sur}^{hyd} \approx R_i + 1 \quad (16)$$

where $d_{total(n-1)}$ and $d_{total(n)}$ denote the distance covered by $\nu^+M^{z+}\nu^-X^{z-}$ at $(n-1)$th and nth steps respectively (at $n = 1$, $d_{total(n-1)} = d_{total}$), while x_n represents the actual displacement of the molecule in the nth step and R_{sur}^{hyd} is the hydrated radius of those molecules that reach the surface of the cube (or) the electrode surface (cf. Scheme 1). Once the molecules reach the electrode surface, they get reduced in a stepwise manner (two electron-transfer reactions ((a) $Cu^{2+} + e \leftrightarrow Cu^+$ and (b) $Cu^+ + e \leftrightarrow Cu$)). Even on the electrode surface the molecules will be slightly hydrated and the water molecules are totally shed after the electron transfer and chemisorption of Cu atoms. The

SCHEME 1: Procedure Employed in the Simulation Technique

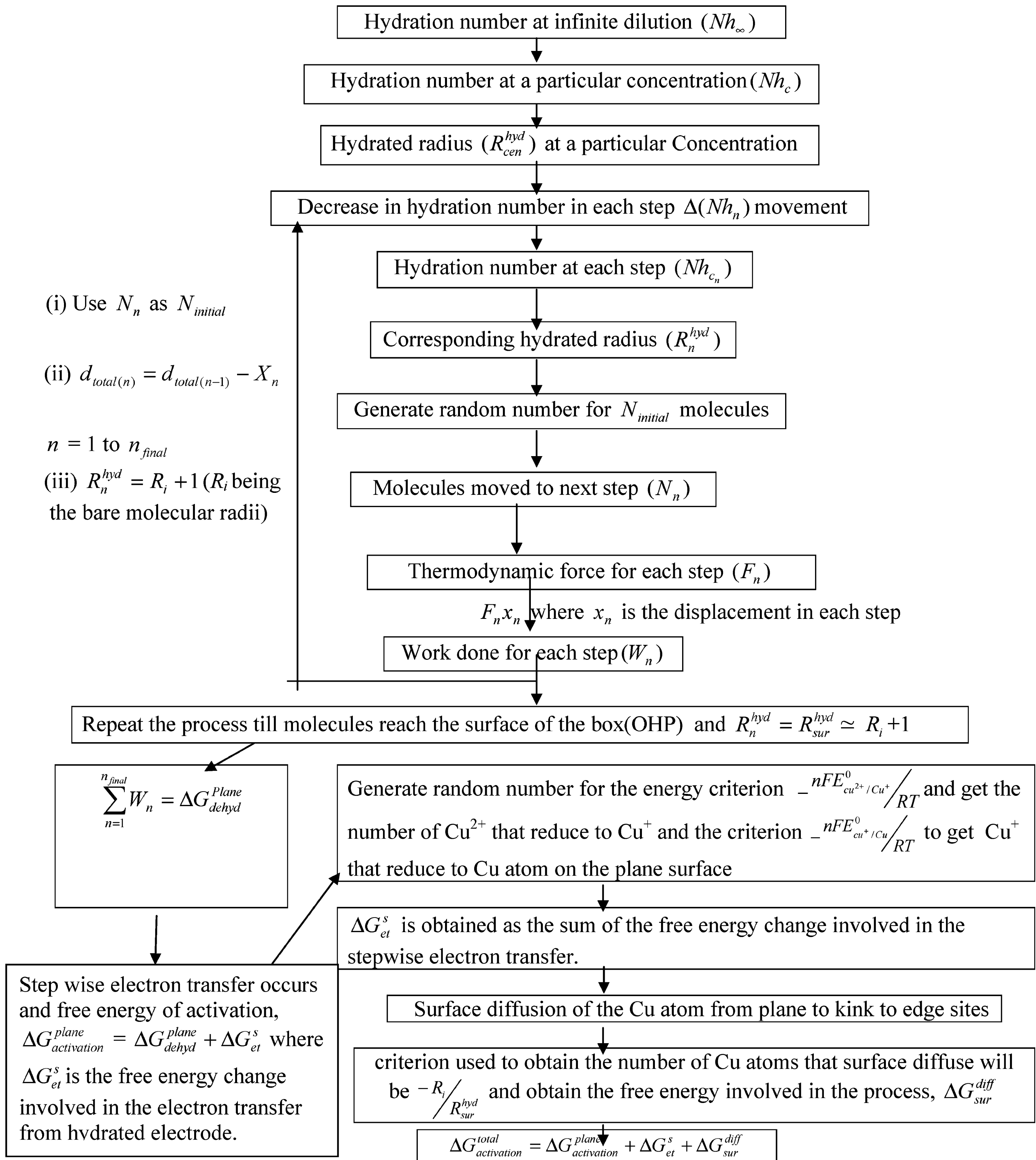

random number criterion for the electron-transfer processes are as follows:

$$ir \geq -nFE^0_{Cu^{2+}/Cu^+}/RT \tag{17}$$

$$ir \geq -nFE^0_{Cu^+/Cu}/RT \tag{18}$$

Here, ir is the random number and $E^0_{Cu^{2+}/Cu^+}$ and $E^0_{Cu^+/Cu}$ denote the standard reduction potential of the Cu^{2+}/Cu^+ and Cu^+/Cu reduction reactions. Those molecules that satisfy conditions (17) and (18) will get reduced and Cu atoms will be formed on the plane sites of the electrode. The free energy change involved in this process along with the dehydration energy leads to the free energy of activation for copper deposition on plane site of the electrode surface, $\Delta G^{plane}_{activation}$. Thus

$$\Delta G^{plane}_{activation} = \Delta G^{plane}_{dehyd} + \Delta G^{s}_{et} \tag{19}$$

where ΔG^{plane}_{dehyd} and ΔG^{s}_{et} represent the free energy change involved in the process of transport of the molecules from bulk

(center of the cube) to the electrode surface via stepwise dehydration and the free energy change for the two, one electron-transfer processes respectively. After the formation of copper atoms on the plane sites, the water molecules surrounding the $CuCl_2$ or $CuSO_4$ are completely shed and the bare Cu atoms start surface diffusion to kink sites and edges of the electrode surface. To account for the number of copper atoms that surface diffuse to kink sites and edges, the criterion $ir \geq -R_i/R_{sur}^{hyd}$ is employed. Here R_i and R_{sur}^{hyd} being the radius of copper atom in vacuum and the hydrated radius of $CuCl_2$ (or $CuSO_4$) molecules when they reached the electrode surface from the center of the cube, respectively. The free energy involved in the surface diffusion is represented as ΔG_{sur}^{diff} and the total free energy of activation involved in the copper deposition at plane, kink and edges of the electrode surface is

$$\Delta G_{activation}^{total} = \Delta G_{activation}^{plane} + \Delta G_{et}^{s} + \Delta G_{sur}^{diff} \quad (20)$$

3.1. Hydration Number and Hydrated Radius at Each Movement of the Molecule. The variation in the hydration number of the ionic pair $\nu_+ M^{z+} \nu_- X^{z-}$ during each movement (ΔNh_n), the hydration number and the hydrated radius in each step (Nh_{c_n} and R_n^{hyd}) are required for obtaining the total number of $CuCl_2$ or $CuSO_4$ molecules that reach the electrode surface. ΔNh_n depends upon (i) the total change in the hydration number of $CuCl_2$ or $CuSO_4$ between infinite dilution and chosen concentration at each step ($\Delta Nh_{total(n-1)} = Nh_\infty - Nh_{c_{(n-1)}}$ and at $n = 1$, $Nh_{c_{(n-1)}} = Nh_c$); (ii) the distance traveled by the hydrated molecule from the center of the cubic box toward the electrode surface ($d_{total(n-1)}$) in each step; and (iii) charges of the ions constituting the ionic pair, concentration of the species, dielectric constant of water.

An exact incorporation of all the above factors is a tedious endeavor; however, a heuristic method of analysis is rendered possible by employing the traditional Debye−Huckel theory (TDH) as applicable to the present simulation procedure. It may be emphasized that improvements to the TDH have been sought in several recent studies so as to describe the electrostatic hole correction terms in a more satisfactory manner.[53] The expression for the classical Debye length is given by[54]

$$L_D = \left(\frac{\epsilon\epsilon_0 k_B T}{(z_+{}^2 + z_-{}^2) N_B e^2}\right)^{1/2} \quad (21)$$

where the dielectric constant of water and permittivity of vacuum are represented by ϵ and ϵ_0, respectively. N_B denotes the number of molecules in the solution and other symbols have their usual significance. In the methodology here, N_B varies at each step on account of the shedding of the hydration sheath progressively, and the expression for the Debye length should reflect this feature. Hence it can be surmised that a discretised Debye length of the form

$$L_{D_{(n-1)}} = \left(\frac{\epsilon\epsilon_0 k_B T}{(z_+{}^2 + z_-{}^2)(N_{(n-1)} + N_{water}) e^2}\right)^{1/2} \quad (22)$$

is appropriate, where n varies from 1 to n_{final}. In eq 22, $L_{D(n-1)}$ denotes the Debye length in the $(n-1)$th step and at $n = 1$, $L_{D_{(n-1)}} = L_D$. $N_{(n-1)}$ denotes the number of electrolyte molecules in the $(n-1)$th step and at $n = 1$, $N_{(n-1)}$ equals the initial electrolyte molecules ($N_{initial}$), N_{water} being the number of water molecules. Further, the variation in the hydration number of the ionic pair is given as

$$\Delta Nh_n = \Delta Nh_{total(n-1)}\left(\frac{L_{D(n-1)} + r_s}{d_{total(n-1)}}\right) \quad (23)$$

At $n = 1$, $\Delta Nh_{total(n-1)} = \Delta Nh_{total}$. Analogously, Nh_{c_n} and R_n^{hyd} can be written as

$$Nh_{c_n} = Nh_{c_{(n-1)}} - \Delta Nh_n \quad (24)$$

and

$$R_n^{hyd} = R_i + \frac{r_s Nh_{c_n}}{\Delta Nh_n} \quad (25)$$

Although eqs 13 and 25 involve the estimation of hydrated radii for the species $CuCl_2$ or $CuSO_4$ at (i) a chosen concentration and (ii) each movement respectively, they are not identical, since eq 13 deals with the total change in the hydration number (ΔNh_{total}) whereas eq 25 is derived for the evaluation of discretised parameter (ΔNh_n). Using the above estimates of Nh_{c_n} and R_n^{hyd} from eqs 24 and 25, the random numbers can be generated for each step. Thus the number of molecules arriving at the surface of the cube and those that subsequently undergo electron transfer are obtained.

3.2. Thermodynamic Force and Associated Energies. If F_n denotes the thermodynamic force and x_n represents the actual displacement of the hydrated electrolyte molecule at the end of the nth step, then W_{total} denotes the total work involved in the displacement of hydrated electrolyte from the center of the cube to the surface, en route to dehydration. In analogy with the definition of the thermodynamic force for continuum models, it is appropriate to write F_n as[56]

$$F_n = \frac{RT(N_{(n-1)} - N_n)}{N_n(R_{n-1}^{hyd} - R_n^{hyd})} \quad (26)$$

where N_n and $N_{(n-1)}$ denote the number of $\nu_+ M^{z+} \nu_- X^{z-}$ molecules present at nth and $(n-1)$th step, respectively, R_n^{hyd} and R_{n-1}^{hyd} being the corresponding hydrated radius and R_{n-1}^{hyd} equals R^{hyd} when $n = 1$. R denotes the universal gas constant, and T refers to the absolute temperature (298 K here). Further, on the basis of considerations emerging from Figure 1, the parametric relation for computing x_n is given by

$$x_n = 2\langle r \rangle \quad (27)$$

The dehydration energy of $CuCl_2$ or $CuSO_4$ follows as:

$$W_{total} = \Delta G_{dehyd}^{plane} = \sum_{n=1}^{n_{final}} w_n = -\sum_{n=1}^{n_{final}} F_n x_n \quad (28)$$

Equation 28 provides the free energy change involved in the transport of the hydrated $CuCl_2$ or $CuSO_4$ molecules from the bulk (center of the cube) to the plane site of electrode surface via dehydration phenomenon.

Copper deposition occurs via two reversible electron-transfer reactions. First electron transfer involves the reduction of Cu^{2+} to Cu^+ and the second is the reduction of Cu^+ to Cu atoms

$$Cu^{2+} + e \leftrightarrow Cu^+ \quad (29)$$

$$Cu^+ + e \leftrightarrow Cu \quad (30)$$

According to the Nernst equation for the electron-transfer processes, the potential at which the reaction occurs can be written as[56]

$$E_{rxn} = E^0_{rxn} + \frac{RT}{nF}\ln\frac{N_{Ox}}{N_{Re\,d}} \quad (31)$$

For reactions 29 and 30, eq 31 can be written as[56]

$$E_{Cu^{2+}/Cu^{+}} = E^0_{Cu^{2+}/Cu^{+}} + \frac{RT}{nF}\ln\frac{N_{Cu^{2+}}}{N_{Cu^{+}}} \quad (32)$$

$$E_{Cu^{+}/Cu} = E^0_{Cu^{+}/Cu} + \frac{RT}{nF}\ln\frac{N_{Cu^{+}}}{N_{Cu}} \quad (33)$$

3.3. Free Energy Change Involved in the Electron-Transfer Process. Equations 32 and 33 provide the electrochemical potential involved in the electron-transfer processes. The terms inside the natural logarithmic function indicates the number of oxidized and reduced species that are involved in the reaction.

To obtain the number of Cu^{2+} that reduces to Cu^{+} on the plane site of the electrode surface, the energy criterion $ir \geq -nFE^0_{Cu^{2+}/Cu^{+}}/RT$ is employed. From the number of Cu^{2+} that reduces to Cu^{+}, the free energy change in each step can be evaluated as follows:

$$E_{Cu^{2+}/Cu^{+}} = E^0_{Cu^{2+}/Cu^{+}} + \frac{RT}{nF}\ln\frac{N_{initial(1)}}{N_{final(1)}} \quad (34)$$

where the standard redox potential[56] $E^0_{Cu^{2+}/Cu^{+}} = -0.18$ V vs SHE, the average of the potential calculated in each seed of random number generation yields the total free energy change involved in the process of electron transfer at the plane site of the electrode surface, $\Delta G^s_{et1} = -nFE_{Cu^{2+}/Cu^{+}}$. $N_{initial(1)}$ is the number of $CuCl_2$ or $CuSO_4$ that reaches the plane surface and $N_{final(1)}$ is the number of Cu^{2+} that is reduced to Cu^{+} at the plane site.

Analogously, for the second reduction reaction, the energy criterion used is $ir \geq -nFE^0_{Cu^{+}/Cu}/RT$ and the energy equation is

$$E_{Cu^{2+}/Cu} = E^0_{Cu^{+}/Cu} + \frac{RT}{nF}\ln\frac{N_{initial(2)}}{N_{final(2)}} \quad (35)$$

In eq 35, $N_{initial(2)} = N_{final(1)}$ i.e. the number of Cu^{+} obtained from the first electron-transfer reaction and $N_{final(2)}$ is the total number of Cu atoms formed from second electron-transfer reaction. $E^0_{Cu^{+}/Cu} = 0.531$ V vs SHE.[56] The average of the potential calculated in each seed of random number generation yields the total free energy change involved in the process of second electron transfer at the plane site of the electrode surface, $\Delta G^s_{et2} = -nFE_{Cu^{+}/Cu}$. Thus the total free energy change involved in the electron-transfer process is given by

$$\Delta G^s_{et} = \Delta G^s_{et1} + \Delta G^s_{et2} \quad (36)$$

Thus

$$\Delta G^{activation}_{plane} = \Delta G^{plane}_{dehyd} + \Delta G^s_{et} \quad (37)$$

The free energy of activation involved in the process of copper deposition at the plane site of the electrode surface can be evaluated from eq 37.

3.4. Free Energy for the Surface Diffusion of Copper Atoms from Plane to Kink to Edge Sites. The random number criterion used to obtain the number of Cu atoms that surface diffuse will be $ir \geq -R_i/R^{hyd}_{sur}$, where R_i and R^{hyd}_{sur} represent the bare crystallographic radius of Cu atoms and the hydrated radius of the $CuCl_2$ or $CuSO_4$ molecules at the electrode surface. This radius ratio is chosen as the criterion for random number generation because, even after the electron-transfer process the anions and water molecules will surround the Cu atoms to initiate the reversible reaction. In order to avoid the reversible reaction, the Cu atoms need to overcome the energy involved in its radius change and surface diffuse to kink and subsequently edge sites of the electrode surface.[57] The justification behind the assumption of ir is provided in section 4.4. The free energy involved in the surface diffusion process is obtained by determining the thermodynamic force that leads to surface diffusion of Cu atoms. The thermodynamic force is calculated as follows:

$$F^{diff}_{sur} = -RTN^{diff}_{sur} \quad (38)$$

where N^{diff}_{sur} denotes the number of Cu atoms that diffuse on the surface of the electrode. The free energy change associated with the surface diffusion of copper atoms from plane to kink to edge sites of the electrode can now be written as

$$\Delta G^{diff}_{sur} = F^{diff}_{sur}(R^{hyd}_{sur} - R_i) \quad (39)$$

From eq 39, the free energy of surface diffusion can be determined. Thus the free energy of activation for the copper deposition process on the plane, kink and edge sites of the electrode surface is now represented as

$$\Delta G^{activation} = \Delta G^{plane}_{activation} + \Delta G^s_{et} + \Delta G^{diff}_{sur} \quad (40)$$

3.5. Influence of the Electric Field. The electron-transfer process from the metal electrode surface to the Cu^{2+} ions in solution is opposed by the presence of the electric field (a vector quantity) at the interface which is normally directed to the interface.[57] Thus the free energy for the reduction of Cu^{2+} ions should include the contribution by the external electric field at the interface. As the Cu^{2+} ions move toward the interface, it has to do some electrostatic work to oppose the electric field present at the interface. If the total potential difference the species passes is ΔE, for the electronation process, the vital part of potential difference the species passes will be written as $\beta\Delta E$. Analogously the free energy for this process can be given as $\Delta G_{ef} = \beta F\Delta E$. The potential difference

$$\Delta E = E_{Cu^{2+}/Cu^{+}} - E_{Cu^{+}/Cu} \quad (41)$$

and the symmetry factor can be written as

$$\beta = \frac{d_{total} - x_n}{d_{total}} \quad (42)$$

where d_{total} is the distance the hydrated molecule should travel from the center of the cubic box to the interface and x_n being the actual displacement of the molecule in each step. Therefore, the total free energy of activation for the electrochemical copper deposition will be

$$\Delta G^{total}_{activation} = \Delta G^{plane}_{activation} + \Delta G^s_{et} + \Delta G^{diff}_{sur} + \Delta G_{ef} \quad (43)$$

Hence by employing eq 43 and random number criteria for each free energy terms, the free energy of activation for copper deposition can be easily evaluated and tedious computation such as KMC techniques, MD simulations are avoided.

4. Results and Discussion

The number of water molecules (N_{water}) is fixed as 18 000. On the other hand, the chosen concentration of the system dictates the number of molecules of copper chloride or copper sulfate ($N_{initial}$). For a chosen concentration, the number of electrolyte molecules and the dimension of the cubic box are estimated by several trial runs of the program by employing the combinations of the two. The particular combination, which satisfies the boundary conditions represented by eqs 15 and 16 is chosen. Since the simulation methodology consumes only a few minutes in the case of 10^2 MC seeds, the above procedure can be done easily. The number of electrolyte molecules, N_{el} varies from 1495 to 4178 for $CuCl_2$ and 1250 to 3322 for $CuSO_4$. The Monte Carlo seeds employed are 10^2, 10^3, 10^4, and 10^5 for each electrolyte. The calculations were carried out using MATLAB version 6.0 on a Pentium IV personal computer. The estimation of the free energy for the whole process of electrochemical copper deposition for each concentration consumes about 14 to 24 h (higher the concentration higher the time) for 10^5 Monte Carlo seeds after the box sizes have been fixed. In several trial runs, the results obtained using 10^5 seeds were not significantly different from that for 10^4 seeds. Consequently, seeds higher than 10^5 were not employed.

4.1. Hydration Behavior of the Electrolyte. As discussed earlier, the first step in the electrochemical copper deposition process is the transport of the hydrated electrolyte molecule from bulk to the metal/electrolyte interface. In each step movement of the hydrated $CuCl_2$ or $CuSO_4$ they shed some of their hydration sheath and accept a new sheath around (configuration change). The number of water molecules shed in each step is determined from the simulation and it was found that as the hydrated molecule reaches the reaction zone it lost almost 99% of its hydration sheath back in the solution. As an illustrative example Figures 3a and 4a and 3b and 4b explain the variation in hydration number and the hydrated radius in each step movement of 6.023×10^{-5} molality of $CuCl_2$ and $CuSO_4$ respectively. Figure 3, panels a and b, explains the shedding of water molecules surrounding the electrolyte, when it moves to next step. This involves breaking of old hydration sheath and subsequent formation of a new one around the electrolyte molecule within the next step movement. This process is very fast because of the excess water molecules present in the solution. Figure 3a shows that $CuCl_2$ requires 6 steps to reach the reaction zone, whereas Figure 3b implies that $CuSO_4$ needs only 4 steps. This could be attributed to the larger size of $CuSO_4$ in comparison with $CuCl_2$. Apart from this, the molecules jump by shedding a larger number of water molecules in the last step due to the electrostatic force at the interface. It is also noticeable that the hydration numbers converge from 10 to 10^5 seeds for both the electrolytes.

As the hydration number of the electrolyte molecules decreases from bulk to the interface, their corresponding hydrated radius also decreases. The Monte Carlo code obeys the criterion given in eqs 15 and 16; hence, the molecules stop moving when they reach the condition $R_n^{hyd} = R_i + 1$, where R_i is the bare crystallographic radius of the molecule under consideration. This condition is imposed on the molecules to ensure that they do not completely dehydrate before reaching the interface. Figure 4, panels a and b, shows the variation in

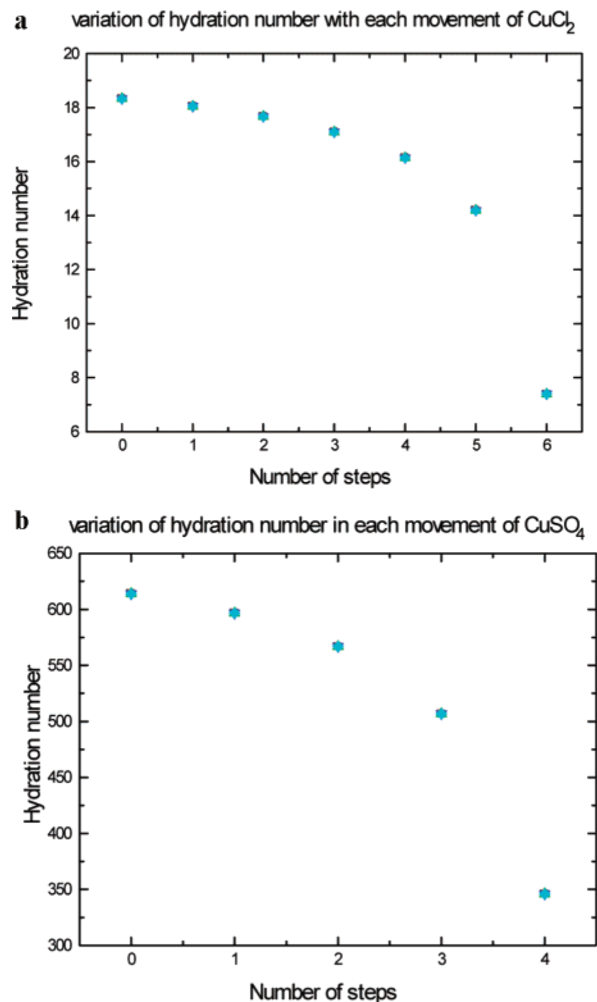

Figure 3. Variation of the hydration number of 6.023×10^{-5} molal solutions of (a) $CuCl_2$ and (b) $CuSO_4$ with their each step movement to reach the reaction zone (metal/electrolyte interface).

the hydrated radius of 6.023×10^{-5} molality of $CuCl_2$ and $CuSO_4$ with the number of movements for all the Monte Carlo seeds employed. From Figure 4, panels a and b, it is clear the hydrated radius decreases in each step movement of the hydrated electrolyte molecule. Although there is a sudden decrease in the hydration number in the last step, the hydrated radius shows gradual decrease. This is due to the decrease in the influence of the secondary and tertiary hydration effects on the electrolyte molecule near the electrode surface.

The dehydration energy can be defined as the free energy required by the hydrated molecule to move from the bulk to the metal/electrolyte interface and is dependent on concentration. The dehydration energy of both hydrated $CuCl_2$ and $CuSO_4$ decreases with increase in concentration. There is a sudden increase in the dehydration energy for concentrations 1.9876 $\times 10^{-4}$ molal and remains almost constant (cf. Figure 5). This anomaly can be explained on the basis of the ion pair formation between the cations and anions of the electrolyte molecule (cf. Figure 6). This behavior is common for electrolytes such as NaCl at concentrations[58] greater than 0.3 M. Figure 5, panels a and b, indicates the variation of the dehydration energy of $CuCl_2$ and $CuSO_4$ with concentration and the Monte Carlo seeds employed. The estimated values of dehydration energies converges for the seeds 10^3, 10^4, and 10^5. From Figures 5 and 6, it is clear that due to ion pair formation, the movement of the hydrated electrolyte molecule and hence the reorganization of hydration is hindered. This hindrance leads to a sudden increase

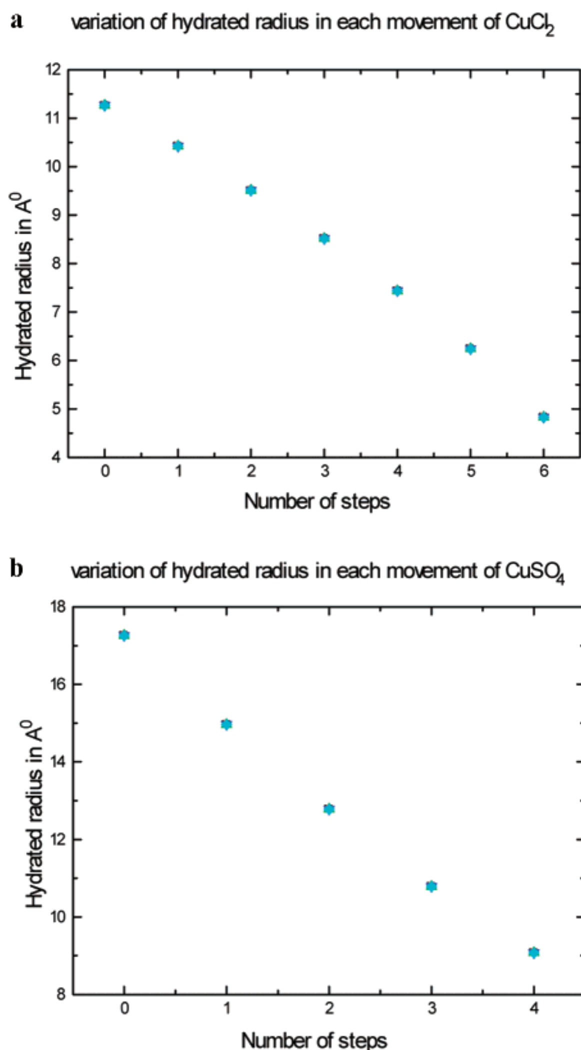

Figure 4. Variation of the hydrated radius of 6.023×10^{-5} molal solutions of (a) $CuCl_2$ and (b) $CuSO_4$ with their each step movement to reach the reaction zone (metal/electrolyte interface).

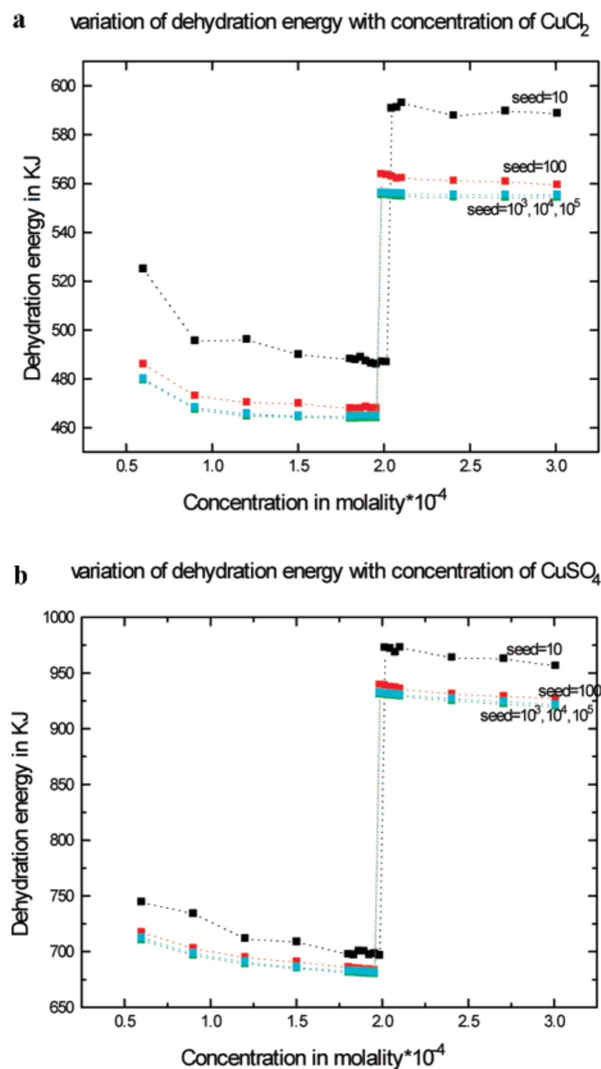

Figure 5. Variation of the dehydration energies of (a) $CuCl_2$ and (b) $CuSO_4$ with the concentration at different Monte Carlo seeds.

in the dehydration energy of both $CuCl_2$ and $CuSO_4$. After a threshold concentration of 2.0177×10^{-4} molal, the dehydration energy remains almost constant for both the electrolyte molecules.

4.2. Free Energy Involved in the Stepwise Electron Transfer from Electrode Surface to the Hydrated Electrolyte Molecule, ΔG^{s}_{et}. In the present case, electron transfer occurs in two steps, first reduction of Cu^{2+} to Cu^{+} occurs and second the reduction of Cu^{+} to Cu atom takes place. In both the processes the reactant species are surrounded by water molecules. There is an equal probability of the reduced species to get oxidized and come back to the solution, the whole process is reversible.[59] Hence, the Nernst equation for the estimation of the equilibrium potential is valid. Employing the Nernst equation, the reduction potential for both the reduction processes are evaluated. The number of oxidized species that gets reduced is obtained from the second set of Monte Carlo codes using the random number criterion $ir \geq -nFE^{0}_{Cu^{2+}/Cu^{+}}/RT$ (to get number of Cu^{2+} that gets reduced to Cu^{+}) and $ir \geq -nFE^{0}_{Cu^{+}/Cu}/RT$ (to get the number of Cu^{+} that reduces to Cu atoms). From these numbers, the equilibrium potential and hence the free energy involved in the process of reduction are calculated. The values of ΔG^{s1}_{et} and ΔG^{s2}_{et} do not change with the concentration of the electrolyte or the seed and remains constant as 17.370 and −50.2765 kJ, respectively. This constant behavior can be attributed to the following two factors: (i) less number of hydrated electrolyte molecule that reaches the metal/electrolyte interface in comparison to the bulk concentration and (ii) the small value of the logarithmic ratio of the number of molecules that reaches the interface to the number that get reduced. Thus, the contribution of the free energy for electron-transfer process to the total free energy of copper deposition is −32.9065 kJ for both $CuCl_2$ and $CuSO_4$.

4.3. Free Energy for Copper Deposition on Plane Site of the Electrode, $\Delta G^{activation}_{plane}$. After the formation of hydrated Cu atoms on the surface of the electrode, deposition of the Cu atoms on the plane site of the electrode occurs. The total free energy involved in the copper deposition on plane site of the electrode is calculated employing eq 37. Figure 7, panels a and b, depicts the trend in the values of $\Delta G^{activation}_{plane}$ with the concentration of the electrolyte employed and the number of Monte Carlo seeds.

The free energies with the concentration of electrolytes and Monte Carlo seeds show identical trends in Figures 5 and 7. Since $\Delta G^{activation}_{plane}$ is defined as the sum of free energy contributions from hydration behavior and electron-transfer process. The value due to second factor (electron transfer) being constant, the values of $\Delta G^{activation}_{plane}$ is totally dominated by the first factor (hydration behavior). The values of $\Delta G^{activation}_{plane}$ decreases with increase in the concentration of the electrolyte and suddenly increase at a value of concentration of 1.9575×10^{-4} molal.

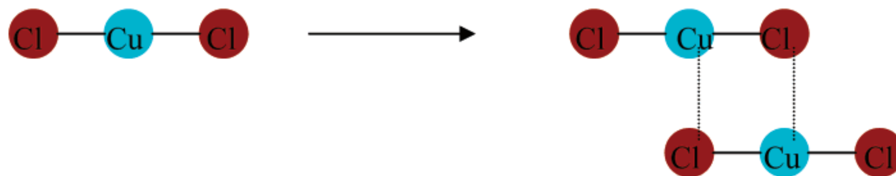

Figure 6. Illustrative example for the ion pair formation between the hydrated $CuCl_2$ molecules at concentrations higher than 1.9575×10^{-4} molal. Here maroon circles denote the hydrated Cl^- ions and blue circles represent the Cu^{2+} ions. Solid lines are covalent bonds and dotted lines depict bonds due to ion pair formation.

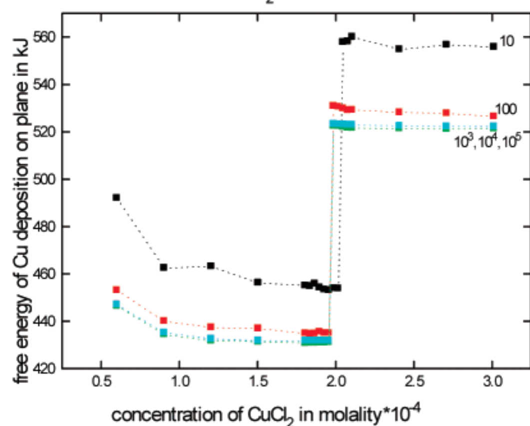

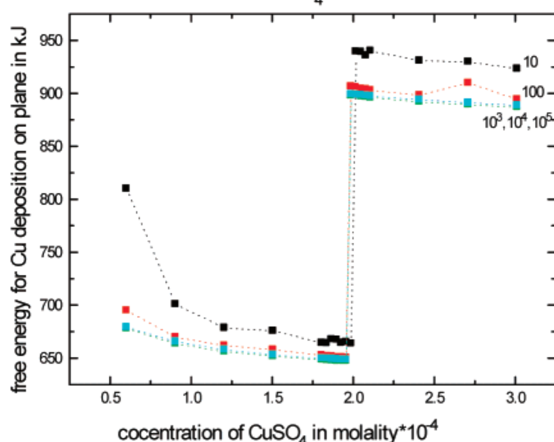

Figure 7. Variation of the free energy for the copper deposition on the plane site of the electrode with concentration of the electrolyte (a) $CuCl_2$ and (b) $CuSO_4$.

After the threshold concentration of 2.0177×10^{-4} molal, $\Delta G^{\text{activation}}_{\text{plane}}$ remains constant. The rationale for this behavior comes from the concept of ion pair formation between the electrolyte molecules with increase in concentration. The ion pairs formed hinder the shedding of water dipoles during the movement of the hydrated $CuCl_2$ or $CuSO_4$ and thereby leading to the sudden jump in $\Delta G^{\text{activation}}_{\text{plane}}$. This leads to the movement of the hydrated molecules as a ion paired entity and not as a single hydrated molecule. The values of $\Delta G^{\text{activation}}_{\text{plane}}$ converges for the MC seeds $>10^2$.

4.4. Surface Diffusion and the Effect of Chloride Ions, $\Delta G^{\text{diff}}_{\text{sur}}$. The hydrated Cu atoms formed on the plane site of the electrode surface moves on the surface of the electrode via diffusion phenomenon. The Cu atoms shed their hydration sheath completely once they get chemisorbed on the edge site of the electrode surface. The free energy involved in the process of surface diffusion of the Cu atoms is estimated by another set of Monte Carlo codes involving the criteria explained in section 3.4 and eq 39. The hydrated radius of $CuCl_2/CuSO_4$ is employed in calculating the random number *ir* for surface diffusion of Cu atoms on the electrode surface rather than the hydrated radius of Cu atom itself. The rationale behind this assumption is that the whole process is reversible and the Cu atoms adsorbed on the electrode surface has equal probability to get oxidized to Cu^+ or Cu^{2+} (into $CuCl_2$ or $CuSO_4$ as the case may be). Apart from this, the oxidized Cu^+ (in the case of $CuCl_2$ as electrolyte) results in an intermediate CuCl that slows down the rate of adsorption of Cu atoms on the electrode surface and lead to the formation of $CuCl_2$. Thus the random number generating criterion should take into account the hydrated radius of the electrolyte species under consideration to explain the effect of concentration of electrolyte on free energy of surface diffusion and to account for the implicit inclusion of the possible formation of a CuCl intermediate during surface diffusion of Cu atoms while simulating the process. As depicted in Figure 8, panels a and b, the free energy for surface diffusion initially increases with increase in the concentration of the electrolyte whereas at the threshold concentration of 2.0177×10^{-4} molal, the value of $\Delta G^{\text{diff}}_{\text{sur}}$ falls suddenly and starts to increase again. As explained in previous sections this behavior of $\Delta G^{\text{diff}}_{\text{sur}}$ with variation in concentration of the electrolyte molecule could be attributed to ion pair formation. As one anticipates, the values of $\Delta G^{\text{diff}}_{\text{sur}}$ for $CuCl_2$ are higher than that of $CuSO_4$. $\Delta G^{\text{diff}}_{\text{sur}}(CuCl_2) \cong 2\Delta G^{\text{diff}}_{\text{sur}}(CuSO_4)$. The higher values of $\Delta G^{\text{diff}}_{\text{sur}}$ for $CuCl_2$ are because of the competitive adsorption between the Cu atoms and the Cl^- ions on the electrode surface. The specific adsorption of the chloride ions on the electrode surface makes the Cu atoms to adsorb on the unoccupied sites of the electrode surface. Thus the Cu atoms have to move a lot on the surface to find a site to get adsorbed. In the case of $CuSO_4$, since ${SO_4}^{2-}$ ions do not adsorb on the electrode surface, the sites are free for the Cu atoms to get adsorbed and hence the value of $\Delta G^{\text{diff}}_{\text{sur}}$ for $CuSO_4$ is less than that of $CuCl_2$. Except the values from MC seed = 10, the $\Delta G^{\text{diff}}_{\text{sur}}$ values converge for 10^2, 10^3, 10^4, and 10^5 for both the $CuCl_2$ and $CuSO_4$.

4.5. Copper Deposition on Plane, Kink, and Edge Sites of the Electrode Surface, $\Delta G^{\text{activation}}$. As discussed in the earlier section, the activation free energy involved in the process of copper deposition on the plane, kink and edge sites of the electrode surface is determined by eq 40. Figure 9 indicates the trend in the values of $\Delta G^{\text{activation}}$ with the concentration of (a) $CuCl_2$ and (b) $CuSO_4$. The values seem to converge for seeds greater than 10^2. From Figure 9, it is clear that, the behavior of $\Delta G^{\text{activation}}$ for $CuCl_2$ is different from that of $CuSO_4$. In the case of $CuCl_2$, the total process of copper deposition is dictated by the surface diffusion, surface diffusion step acts as the rate determining step and hence Figure 9a is identical in trend to that of Figure 8a. This is due to higher values of $\Delta G^{\text{diff}}_{\text{sur}}$ for $CuCl_2$, because of the competitive adsorption between chloride ions and Cu atoms on the electrode surface. Figure 9b indicates that, the whole process of copper deposition is governed by the

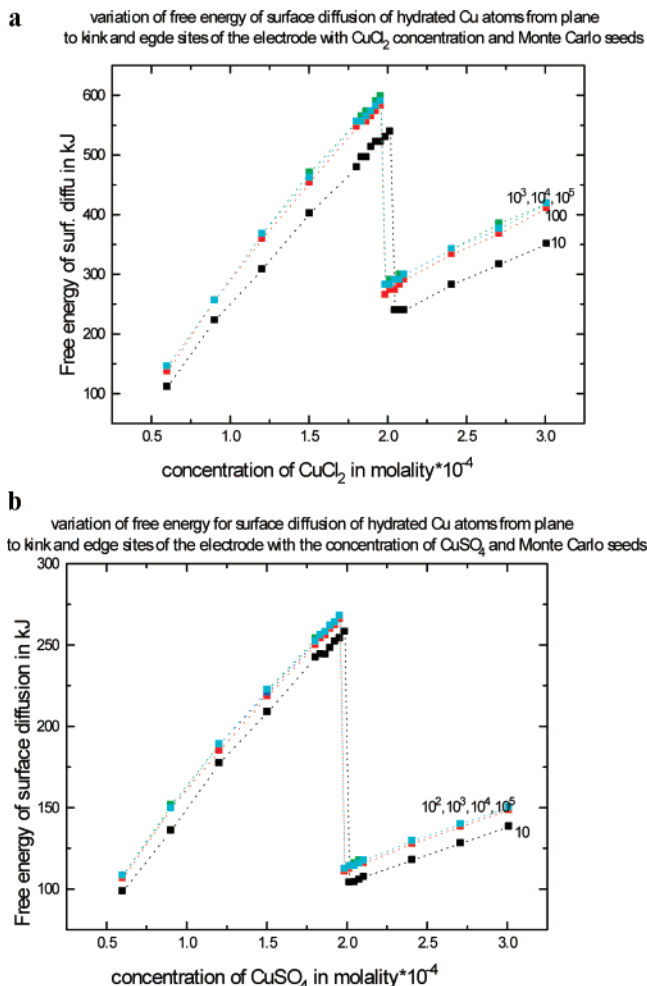

Figure 8. Variation of the free energy involved in the surface diffusion of hydrated Cu atoms from plane to kink and edge sites of the electrode surface (a) $CuCl_2$ and (b) $CuSO_4$.

transport of the hydrated $CuSO_4$ molecules from bulk to the metal/electrolyte interface. In the case of $CuSO_4$, mass transport of the hydrated electrolyte molecule acts as the rate determining step and hence Figure 9b is identical to Figure 7b. Thus the present simulation methodology in addition to evaluating the free energy of activation for copper deposition also predicts the rate determining step for the process. The value of $\Delta G^{\text{activation}}$ at seed = 10 shows more deviation whereas other seeds converge and hence seeds higher than 10^5 are not employed.

4.6. Presence of Electric Field. In section 3.5, the evaluation of free energy contribution due to the presence of external electric field was discussed. Equations 41 and 42 are employed for this purpose. The values of ΔG_{ef}, evaluated from these equations, increase with increase in the concentration of the electrolyte molecule. ΔG_{ef} ($CuCl_2$) < ΔG_{ef} ($CuSO_4$). Table 1 represents the variation of ΔG_{ef} with the concentration of $CuCl_2$ and $CuSO_4$. The values of ΔG_{ef} converges for all Monte Carlo seeds and hence those values corresponding to the 10^5 seed are tabulated. Table 1 implies that ΔG_{ef} for $CuSO_4$ is nearly twice that of $CuCl_2$. This can be rationalized on the basis of the difference in molecular size between $CuCl_2$ and $CuSO_4$. From section 4.1, it is clear that $CuSO_4$ due to its larger size takes fewer steps to reach the interface whereas $CuCl_2$ takes more steps. Thus the value of the symmetry factor β is more for $CuSO_4$ and as a result that of ΔG_{ef}.

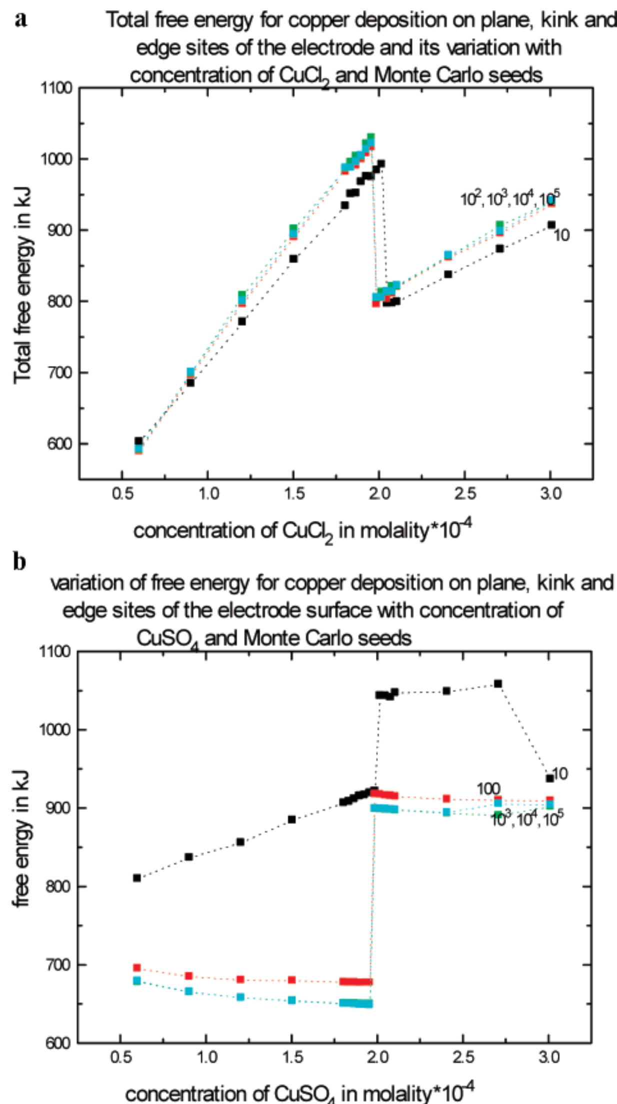

Figure 9. Variation of the free energy for the copper deposition on the plane, kink, and edge sites of the electrode surface with the concentration of the electrolytes and the Monte Carlo seeds.

TABLE 1: Free Energy for Copper Deposition in the Presence of Electric Field

S. no	concentration in molality $\times 10^{-4}$	ΔG_{ef} in kJ at seed = 10^5	
		$CuCl_2$	$CuSO_4$
1.	0.6023	27.1343	52.4593
2.	0.90345	27.6903	53.2043
3.	1.2046	28.0245	53.6191
4.	1.5057	28.2521	53.8861
5.	1.8069	28.4193	54.0723
6.	1.8376	28.4339	54.0879
7.	1.8677	28.4479	54.0981
8.	1.8978	28.4615	54.1178
9.	1.9280	28.4748	54.1318
10.	1.9575	28.4875	54.1460
11.	1.9876	28.5002	54.1593
12.	2.0177	28.5126	54.1725
13.	2.0478	28.5247	54.1853
14.	2.0779	28.5365	54.1978
15.	2.1074	28.5478	54.2102
16.	2.4098	28.6511	54.3164
17.	2.7110	28.7353	54.4012
18.	3.0121	28.8058	54.4700

4.7. Total Free Energy of Activation for Electrodeposition of Copper, $\Delta G^{\text{total}}_{\text{activation}}$. Since $\Delta G^{\text{total}}_{\text{activation}}$ is the sum of contributions from the free energies of various processes that lead to

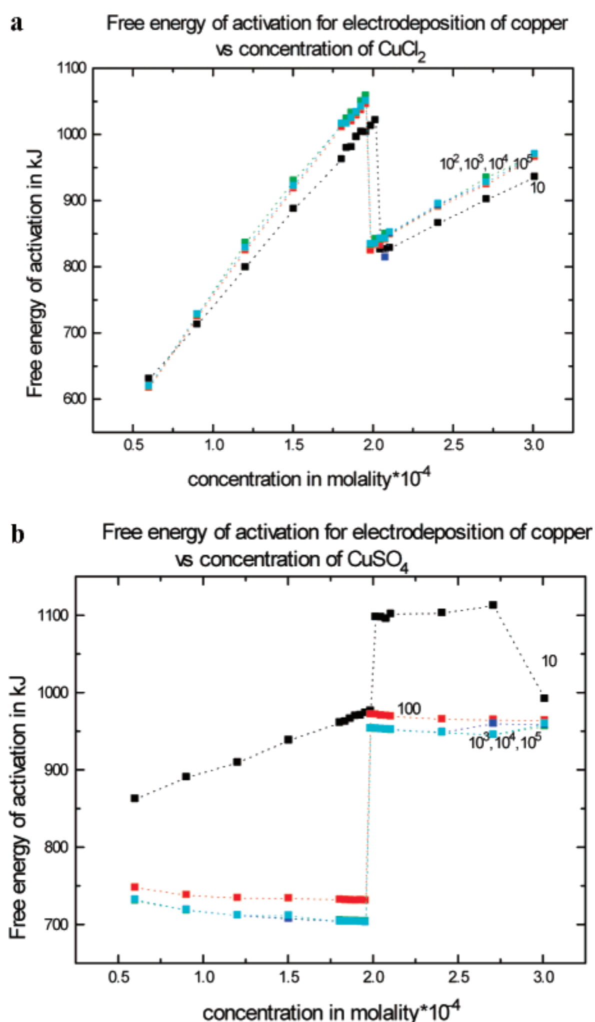

Figure 10. Variation of the free energy of activation for the electrodeposition of copper with the concentration of the electrolytes and the Monte Carlo seeds.

copper deposition on electrode surface, Figures 9a and 10a are similar whereas Figures 9b and 10b are identical. It is clear from eq 43 and Figure 10 that $\Delta G_{\text{activation}}^{\text{total}}$ is dominated by surface diffusion of Cu atoms for $CuCl_2$, while mass transport of hydrated electrolyte molecule dictates $\Delta G_{\text{activation}}^{\text{total}}$ for $CuSO_4$. Thus, step I, the dehydration and movement of hydrated $CuSO_4$ molecules from bulk to metal/electrolyte interface becomes the rate determining step for electrodeposition of copper from $CuSO_4$ solution and step III, the surface diffusion of hydrated Cu atoms on the surface of electrode becomes the rds for electrodeposition of copper from $CuCl_2$, due to competitive chloride ion specific adsorption on the electrode surface.[60] The formation of intermediate CuCl affects the rate of electrodeposition of copper from $CuCl_2$ significantly. Although this process of formation of CuCl is not explicitly incorporated in the simulation codes, the fact is implicitly taken into account via the assumption of reversible oxidation of Cu atoms to CuCl and then $CuCl_2$ on the electrode surface. Thus the free energy of activation for copper electrodeposition from $CuCl_2$ rises steeply unlike $CuSO_4$. As the concentration of $CuCl_2$ increases due to adsorption of Cu atoms, Cl^- concentration is more in solution, thereby facilitating the CuCl intermediate formation and lowering the rate tremendously (cf. Figures 9a and 10a).

5. Perspectives

The foregoing analysis has provided a simple framework whereby the energetics involved in the electrodeposition of copper can be computed efficiently. Several parameters such as the extent of variation of hydration numbers, mean nearest neighbor distances, discretized "Debye length", etc. are introduced and expressed parametrically, invoking the validity of hard sphere assumption in conjunction with intuitive chemical principles. In contrast, the hitherto-existing Monte Carlo and molecular dynamic approaches for the estimation of free energy of activation and related parameters are based on conceptually solid foundations insofar as they incorporate exact potential functions, electrostatic effects and time-constants associated with the process. However, these are computationally tedious. In the present study, the formalism has been found to be valid for copper deposition from $CuCl_2$ and $CuSO_4$ solutions and several subtle features regarding the importance of using these electrolytes on the rate of the reaction are pointed out. However, it can be reiterated that this formalism is essentially of a complementary nature to the existing literature[61,62] on electrodeposition of copper and can easily be extended to investigate the presence of organic additives in the phenomenon of copper deposition. While a detailed critique is warranted in order to obtain a comprehensive perspective, it is noteworthy that an alternate treatment of electrodeposition of copper based on hydration behavior of electrolytes is indeed plausible. The methodology itself is novel and different from other models reported in the literature. It involves continuum model in solution via modified Debye length, change in hydrated radii and hydration number in each point of motion of the molecule, change in concentration at each point, $\partial c/\partial x$, whereas other methodologies are based on Concentrated solution theory, CST. The present simulation is time independent because, it explains only the process of initial copper electrodeposition on the edge site and not the further growth and nucleation, but these two processes can be simulated with addition of few more steps in the existing code, which could be a separate work of significance. Apart from this the electrode surface is assumed to be anisotropic and hence no parameters of the metal electrode are being introduced. This makes the present simulation continuum in solution and considering the electrode surface only as an electron source or sink. When the metallic parameters like effect of anisotropy, porosity of the electrode comes in to picture, this work will become multi scale in nature. This can be done with certain significant variation in the present simulation code by introducing (i) time dependency, (ii) connecting the free energy of activation to the flux via expression involving $\partial c/\partial x$ and thermodynamic force etc as a future improvement in the methodology.

6. Conclusions

The step wise free energy involved in the process of electrochemical copper deposition is estimated employing a multistep continuum Monte Carlo simulation technique. The hydrated radii, bare radii, and hydration number of the species ($CuCl_2$ or $CuSO_4$ or Cu as the case may be), is used to obtain the number of species via random number generation. The effect of concentration of the electrolyte, influence of the electric field and presence of chloride ions on the free energy for the processes involved in the copper deposition is studied. The plausible rate determining step for the process of electrodeposition of copper from $CuCl_2$ and $CuSO_4$ was determined.

Acknowledgment. The authors gratefully thank the reviewers for their helpful comments and the U.S. Government for supporting this work.

References and Notes

(1) Kesmodel, L. L.; Falicov. L. *Solid State Commun.* **1975**, *16*, 1201.

(2) Vereecken, P.; Binstead, R.; Deligianni, H.; Andricacos, P. *IBM J. Res. Develo.* **2005**, *49*, 3.

(3) Price, D. L.; Halley, J. *J. Chem. Phys.* **1995**, *102*, 6603.

(4) Romankiw, L. T.; Croll, I.; Hatzakis, M. *IEEE Trans. Mag.* **1970**, *MAG-3*, 597.

(5) Löchel, B.; Maciossek, A.; König, M.; Huber, H-L.; Bauer, G. *Microelectron. Eng.* **1993**, *21*, 463.

(6) Yang, F. Y. *Science* **1999**, *284*, 1335.

(7) Barrett, J. J.; Smits, E. M.; Moran, P. L. *Proc. Integrated Circuit Technology Conf.* **1986**.

(8) Andricacos, P. C. *IBM J. Res. Develop.* **1998**, *42*, 567.

(9) Datta, M. *IBM J. Res. Develop.* **1998**, *42*, 563.

(10) Löchel, B.; Maciossek, A.; Quenzer, H. J.; Wagner, B. *J. Electrochem. Soc.* **1996**, *143*, 237.

(11) Li, C. Z.; Tao, N. J. *Appl. Phys. Lett.* **1998**, *72*, 894.

(12) Morpurgo, A. F.; Marcus, C. M.; Robinson, D. B. *Appl. Phys. Lett.* **1999**, *74*, 2084.

(13) Li, C. Z.; Bogozi, A.; Huang, W.; Tao, N. J. *Nanotechnology* **1999**, *10*, 221.

(14) Mingshaw, W. W.; Lydia, L. S. *IEEE Elec. Device Lett.* **2000** 21

(15) Lingk, C.; Gross, M. E. *J. Appl. Phys.* **1998**, *84*, 5547.

(16) Krongelb, S.; Romankiw, L. T.; Tornello, J. A. *IBM J. Res. Develop.* **1998**, *42*, 575.

(17) Batinat, N.; Kolb, D. M. *Langmuir* **1992**, *8*, 2572.

(18) Edelstein, D. C.; Andricacos, P. C.; Agarwala, B.; Carnell, C.; Chung, D.; Cooney, E., III.; Cote, W.; Locke, P.; Luce, S.; Megivern, C.; Wachnik, R.; Walton, E. *Electrochem. Soc. Proc. Ser.* **1999**, *99−9*, 1.

(19) Başol, B.; Uzoh, C.; Talieh, H.; Wang, T.; Guo, G.; Erdemli, S.; Mai, D.; Lindquist, P.; Bogart, J.; Cornejo, M.; Cornejo, M.; Basol, E. *The National AIChE Meeting*, San Francisco CA. Nov. 17−18, 2003.

(20) Andricacos, P. C. *Electrochem. Soc. Interface* **1999**, *8*, 32.

(21) Harper, J. M. E.; Cabral, C., JR.; Andricacos, P. C.; Gignac, L.; Noyan, I. C.; Rodbell, K. P.; Hu, C. K *J. Appl. Phys.* **1999**, *86*, 2516.

(22) Budevski, E.; Staikov, G.; Lorenz, W. J. *Electrochemical Phase Formation and Growth*; VCH: Weinheim, Germany, 1996.

(23) Dini, J. W. In *Modern Electroplating*, 4th ed.; Schlesinger, M.; Paunovic, M., Eds.; Wiley: New York, 2000.

(24) Andricacos, P. C.; Uzoh, C.; Dukovic, J. O.; Horkans, J.; Deligianni, H. *IBM J. Res. Develop.* **1998**, *42*, 567.

(25) Nikolic, N. D.; Popov, K. I.; Pavlovic, L. J.; Pavlovic, M. G *Sensors* **2007**, *7*, 1.

(26) Cheol, S. H.; Dong, J.; Liu, M. *Adv. Mater.* **2003**, *15*, 1610.

(27) Dima, G. E.; de Vooys, A. C. A.; Koper, M. T. M. *J. Electroanal. Chem.* **2003**, *554−555*, 15.

(28) Pletcher, D.; Poorbedi, Z. *Electrochim. Acta* **1979**, *24*, 1253.

(29) Grujicic, D.; Pesic, B. *Electrochim. Acta* **2005**, *50*, 4426.

(30) Grujicic, D.; Pesic, B. *Electrochim. Acta* **2002**, *47*, 2901.

(31) Danilov, A. I.; Molodokina, E. B.; Yu, M. Polukarov *Russ. J. Electrochem.* **2002**, *38*, 732.

(32) Danilov, A. I.; Molodokina, E. B.; Baitov, A. A.; Pobelov, I. V.; Yu, M. Polukarov *Russ. J. Electrochem.* **2002**, *38*, 836.

(33) Oskam, G.; Vereecken, P. M.; Searson, P. C *J. Electrochem. Soc.* **1999**, *146*, 1436.

(34) Radisic, A.; Long, J. G.; Hoffmann, P. M.; Searson, P. C *J. Electrochem. Soc.* **2001**, *148*, C41.

(35) Drews, T. O.; Webb, E. G.; Ma, D. L.; Alameda, J.; Braatz, R. D.; Alkire, R. C *AIChE J.* **2004**, *50*, 1.

(36) Pricer, T. J.; Kushner, M. J.; Alkire, R. C. *J. Electrochem. Soc.* **2002**, *149*, C396.

(37) Scharifker, B.; Hills, G. *Electrochim. Acta* **1983**, *28*, 879.

(38) Drews, T. O.; Braatz, R. D.; Alkire, R. C. *Intl. J. Multiscale Comput. Eng.* **2004**, *2*, 313.

(39) Drews, T. O.; Webb, E. G.; Ma, D. L.; Alameda, J.; Braatz, R. D.; Alkire, R. C. *AIChE J.* **2004**, *50*, 226.

(40) Gillespie, D. *J. Chem. Phys.* **2001**, *115*, 1716.

(41) Cao, Y.; Gillespie, D.; Petzold, L. *J. Chem. Phys.* **2006**, *124*, 044109.

(42) Yang, Y. G.; Johnson, R. A.; Wadley, H. N. G. *Acta Mater.* **1997**, *45*, 1455.

(43) Huang, H.; Filmer, G. H.; Diaz de la Rubia, T. *J. Appl. Phys.* **1998**, *84*, 3636.

(44) Wang, L.; Clancy, P. *Surf. Sci.* **2001**, *473*, 25.

(45) Gilmer, G. H.; Huang, H.; Tomas, Diaz de la Rubia; Torre, J. D.; Baumann, F. *Thin Solid Films* **2000**, *365*, 189.

(46) Pomeroy, J. M; Jacobsen, J; Colin C; Cooper, B. H.; Sethna, J. P. *Phys. Rev B* **2002**, *66*, 235412.

(47) Liu, C. L.; Cohen, J. M.; Adams, J. B.; Voter, A. F. *Surf. Sci.* **1991**, *253*, 334.

(48) Stumpf, R.; Scheffler, M. *Phys. Rev. B* **1996**, *53*, 4958.

(49) Coronell, D. G.; Hansen, D. E.; Vorter, A. F.; Liu, C. L.; Liu, X. Y.; Kress, J. D. *Appl. Phys. Lett.* **1998**, *73*, 3860.

(50) Liu, Z.-l; Yu, L.; Yao, K.-l; Jing, X.-b; Li, X.-a.; and X-a.; Sun, X.-z. *J. Phys. D: Appl. Phys.* **2005**, *38*, 4202.

(51) Harinipriya, S.; Sudha, V.; Sangaranaryanan, M. V. *Langmuir* **2004**, *20*, 1871.

(52) Bockris, J. O'M.; Conway, B. E *Modern Aspects of Electrochemistry*; Academic Press, Inc.: New York 1954; Vol. 1, Chapter 1.

(53) See for example, Shklovskii, B. I.; Eforos, A. L. *Electronic properties of doped semiconductors*; Springer−Verlag: New York, 1984.

(54) Faules Fritsch, I.; Faulkner, R. L. A. *J. Electroanal. Chem.* **1989**, *263*, 237.

(55) Mclendon, G.; Miller, J. R. *J. Am. Chem. Soc.* **1985**, *107*, 7811.

(56) Atkins, P. W. *Physical Chemistry*, 5th ed.; Oxford Univ. Press: New York, 1994.

(57) Bockris, J. O'M.; Reddy, A. K. N *Modern Electrochemistry*; Plenum Press, Inc.: New York, 1977; Vol. 2, Chapter 8.

(58) Marti, J.; Csajka, F. S. *J. Chem. Phys.* **2000**, *113*, 1154.

(59) Bockris J. O'M.; Reddy, A. K. N. *Modern Electrochemistry*; Plenum Press, Inc.: New York, 1977; Vol. 2, Chapter 10.

(60) Dow, W.-P.; Huang, H.-S.; Yen, M.-Y.; Chen, H.-H. *J. Electrochem. Soc.* **2005**, *152*, C77.

(61) Li, X.; Drews, T. O.; Rusli, E.; Xue, F.; He, Y.; Braatz, R. D.; Alkire, R. C. *J. Electrochem. Soc.* **2007**, *154*, D230.

(62) Rusli, E.; Xue, F.; Drews, T. O.; Vereecken, P.; Andracacos, P.; Deligianni, H.; Braatz, R. D.; Alkire, R. C. *J. Electrochem. Soc.* **2007**, *154*, D584.